Journal of Contemporary Urban Affairs

2023, Volume 7, Number 2, pages 37–55

*Original scientific paper*

# Urban Heat Island Impact and Precipitation Patterns in Indian Western Coastal Cities

*[1] Ph.D **Rachana Patil** , [2] Asst. Prof. Dr. **Meenal Surawar**

[1] Department of Architecture and Planning, Research Scholar, Visvesvaraya National Institute of Technology, India

[2] Department of Architecture and Planning, Faculty of Architecture, Visvesvaraya National Institute of Technology, India

[1] E-mail: da22arc005@students.vnit.ac.in , [2] E-mail: meenalsurawar@arc.vnit.ac.in

**ARTICLE INFO:**

**Article History:**
Received: 26 August 2023
Revised: 19 November 2023
Accepted: 12 November 2023
Available online: 11 November 2023

**Keywords:**
Urban Heat Island,
Population Density,
Precipitation Patterns,
Coastal Urbanization,
Climate Change,
Western Coastal Cities.

This article is an open-access article distributed under the terms and conditions of the Creative Commons Attribution 4.0 International (CC BY 4.0)

**Publisher's Note:**
Journal of Contemporary Urban Affairs stays neutral with regard to jurisdictional claims in published maps and institutional affiliations.

**ABSTRACT**

*This article investigates the Urban Heat Island (UHI) effect and its interplay with precipitation patterns in the rapidly urbanizing western coastal cities of India. Focusing on the socio-economic dimensions of urbanization, it examines the consequences of increased surface temperatures due to altered urban landscapes and heightened anthropogenic activities. The study evaluates the correlations between UHI intensity, population density, and precipitation during summer and winter across multiple decades—1991, 2001, 2011, and 2021—using the Spearman rank correlation coefficient. Findings indicate a robust positive correlation between surface temperature and population density in summer, with an inverse relationship to precipitation. In contrast, winter data shows an opposite trend, with unclear connections to population density, suggesting that other factors may significantly affect precipitation. The seasonal and temporal analysis of these correlations sheds light on the urban climate's complexity and informs urban planning strategies to mitigate adverse socio-economic impacts related to climate change. This study underscores the need for sustainable urban development practices that consider the intricate dynamics between urban growth and environmental transformations, highlighting the necessity for climate-responsive planning in the socio-economic development of Indian western coastal cities.*

JOURNAL OF CONTEMPORARY URBAN AFFAIRS (2023), ***7***(2), 37-55.
https://doi.org/10.25034/ijcua.2023.v7n2-3

www.ijcua.com

Copyright © 2023 by the author(s).

| **Highlights:** | **Contribution to the field statement:** |
|---|---|
| In Indian Western Coastal Cities"<br>- There is a noteworthy and progressively strengthening positive relationship observed between surface temperature and population density during the summer season. However, during the winter season, there is an insignificant negative correlation observed.<br>- In the case of surface temperature and precipitation, their relationship is negative during the summer and positive during the winter.<br>- The link between population density and precipitation is unclear and inconsistently weak, suggesting other factors may influence precipitation more significantly. | The research presented in this article is pertinent to socio-economic aspects of urbanization as it provides critical insights into how the UHI effect, driven by population concentration, can exacerbate climate-related challenges such as heatwaves and flash floods. These environmental changes have direct implications on public health, urban infrastructure, and the overall quality of life, influencing socio-economic disparities. The study's conclusions can aid policymakers and urban planners in devising strategies to create more sustainable and resilient urban spaces, ultimately contributing to more equitable socio-economic development in the context of rapid urbanization. |

***Corresponding Author:**
Department of Architecture and Planning, Research Scholar, Visvesvaraya National Institute of Technology, India
Email address: da22arc005@students.vnit.ac.in

**How to cite this article:**
Patil, R., & Surawar, M. (2023). Urban Heat Island Impact and Precipitation Patterns in Indian Western Coastal Cities. *Journal of Contemporary Urban Affairs*, 7(2), 37-55. https://doi.org/10.25034/ijcua.2023.v7n2-3

## 1. Introduction

Due to increasing development, urbanization is increasing at a rapid scale. As a result, cities are expanding in terms of area and population density. Due to this, built-up area replaces green areas (Malik & Gupta, 2018). As per distribution all over the world, Indian cities exhibited higher densities. India has a smaller share of the world's habitable land mass, about 2.4%, than its population share, which is 18% (Sarbapriya & Ishita, 2011). India's ability to accommodate such a large population on a limited area of land is advantageous because it causes less harm to the natural ecology, but it has many negative effects. One such consequence is urban heat islands. Urban Heat Island exhibits a positive relationship with population density (Oke T. R., 1973; Arifwidodo & Chandrasiri, 2015). Urban heat islands increase as the number of people living per unit area increases. In countries like India, where the densities are already high, it has many negative impacts, such as an increase in discomfort and energy demand, etc. during the summer season (Nuruzzaman, 2015). Several studies have demonstrated a direct relationship between temperature and the daily death rate as the risk of heat-related morbidity and mortality increases (Tan et al., 2010; Gabriel & Endlicher, 2011; Habeeb et al., 2015; Golechha et al., 2021).

The Urban heat island is a phenomenon in which a city experiences higher temperatures than its surrounding rural areas. Luke Howard initially investigated and described this phenomenon in the 1810s. According to Luke Howard, London's downtown area was 2.1 °C (3.7 °F) warmer at night than the surrounding countryside (Mills, 2016). The causes of urban heat islands can be divided into two main categories: natural factors, which encompass urban geography, global climate, and local weather conditions, that are beyond human control. Anthropogenic factors such as city size, human activities, city layout, $CO^2$ emissions, heat absorption caused by low albedo materials, heat retention in the atmosphere due to air pollutants and urban canopy, reduced convection due to wind obstruction by urban structures, decreased cooling efficiency due to the loss of trees, and heat discharge into the atmosphere from the use of air conditioners, machinery, and vehicles, among other factors, which can be controlled (Nuruzzaman, 2015; Wai et al., 2022). These anthropogenic factors cause changes in net radiation because of a reduction in short-wave solar radiation and incident flux re-emission of long-wave radiation by the urban surface. This is absorbed by the atmosphere and it warms the air (Oke et al., 2017). The main reason for this is that urban areas are increasing, and the pervious surfaces are converted to impervious surfaces. As per various studies, 9 $m^2$ of green space is required per person (Russo & Cirella, 2018). However, places like Mumbai have less green space per person at 0.12 $m^2$ (Hwang et al., 2020). Therefore, the rate of evaporative cooling is reduced in the case of urban areas. This raises the temperature in the urban area by heating it (Oke et al., 2017). UHI can be broadly classified as boundary level UHI, which is related to the weather at the mesoscale; canopy layer UHI, which is a near-surface air layer that extends from the ground to the mean building height; and surface UHI, which, is related to land surface temperature (Martin et al., 2015). The land surface temperature that influences surface UHI is the primary focus of this research.

Recently, there has been a noticeable shift in conventional seasonal patterns. An escalation is observed in the occurrence of unforeseen precipitation during periods that were historically non-rainy, and a notable increase in the frequency of heat waves. These climatic shifts have consequently led to increased discomfort within urban locales. Complicating matters further is the accelerating pace of urbanization, which amplifies people's exposure to these unpredicted events (Xiao et al., 2017). Consequently, there exists a compelling need to investigate the intricate interplay between population, surface temperature, and precipitation patterns, particularly during the non-rainy season.

### *1.1.UHI and Population*

The seasonal and temporal distribution of UHI and the effects of various factors on UHI have been highlighted over the past few decades. Since 1937, researchers have noted rising air temperature values in cities, which they have linked to an increase in population and the rapid increase in infrastructure development in the urban environment in response to the increasing demands (Oke T. R., 1973; Oke & Maxwell, 1975; Li et al., 2020). When the graph of the population density and UHI is plotted, a direct association is seen (Mallick, 2021). Within the urban area where the population density and building density are high and green cover is less, records the highest mean air temperature. (Kotharkar & Surawar,

2016). UHI is highly correlated with building height and urban fraction, which affect canopy UHI and surface UHI, respectively. (Li, Y., et al., 2020). When compared over time, areas that have changed from vegetated to non-vegetated areas to accommodate an increase in the population show a significant temperature shift (Zhou & Wang, 2011). To study the dynamics of land use and land cover change over time, researchers use land use indices such as the normalized difference built-up index (NDBI), normalized difference bareness index (NDBaI), and normalized difference vegetation density index (NDVI), which signifies built-up land, bare land, and vegetation, respectively. NDVI is indirectly proportional to UHI, implying that as vegetation cover increases, UHI decreases, NDBI and NDBaI are directly proportional to UHI, indicating that as built-up area and bare land increase, UHI increases (Tran, et al., 2017). When the relationship between UHI and land use indices was studied over a period of time, it was observed that the slope of UHI and NDVI decreased, but that of UHI and NDBI, NDBaI increased (Pal & Ziaul, 2017; Ogunjobi et al., 2018; Dissanayake et al., 2019; Das, et al., 2020;). This shows that over time, due to rapid population growth, green spaces are being converted to built-up regions, which has exacerbated UHI. Population density alters urban form in terms of land cover and morphology. In the case of land cover, as urbanization increases, green cover reduces, and in the case of urban morphology, it reduces the permeable surface fraction that increases UHI (Ramírez-Aguilar & Lucas Souza, 2019) which triggers the UHI. However, this relationship may vary from city to city because of variations in density, urban geography, urban setting, and the heat capacity of the urban fabric (Louiza et al., 2015). Therefore, the investigation of this relationship must be tailored to the specific spatial context.

### *1.1.1. UHI and Urban Geography*

Urban geography impacts UHI. The effect of UHI is different for coastal cities than for inland cities. Urban geography and climate zones play an important role in influencing UHI (Sarkar et al., 1998; Simpson et al., 2008). Depending on the urban geography, UHI shows seasonal variation. The variations are distinct in Inland and coastal cities from those in mountainous areas and polar cities. In coastal cities, the presence of sea/land breeze interaction enhances the cooling effect, which reduces UHI (Yamato et al., 2017; Matsumoto et al., 2017). The absence of sea breeze interaction in Inland cities reduces the cooling effect, thus increasing UHI (Ramamurthy & Zeid, 2017). However, although coastal cities stayed colder than inner city areas during the day, the opposite happened at night as the sea takes a long time to heat up and cool down. Cities in mountainous areas have wind valley systems that consist of up valley winds during the day and shallower winds coming down from mountains during the night, which reduces the impact of UHI (Ketterer & Matzarakis , 2014). In polar cities, snow's insulating capabilities minimize heat storage and the demand for residential heating (Leroyer et al., 2010). In addition, the radiation balance and energy exchanges are further impacted by the snow cover and melting processes, which reduces the latent heat flux (Karsisto et al., 2016). Additionally, polar cities have lower population densities than other cities; hence, the effect of UHI is often less noticeable there. (Leroyer et al., 2010). Urban geography impacts how UHI affects cities, as coastal and inland areas experience seasonal variations in UHI. This research focuses on tier 2 cities within the Western Coastal Region of India, analyzing correlations between the study parameters within a similar category of cities to reduce the impact of outliers.

### *1.2.UHI and Precipitation*

Precipitation can be categorized into two main types: convective precipitation and stratiform precipitation (Houze, 1989). Convection precipitation occurs when the Earth's surface, particularly in an unstable or moist atmosphere, experiences greater heating than its surrounding environment. This heightened heating leads to substantial evapotranspiration, resulting in precipitation. Convection precipitation is characterized by its limited spatial coverage, intense upward motion caused by local heating, and high precipitation intensity. Stratiform precipitation occurs when large-scale winds and atmospheric dynamics force large air masses to move over each other. This type of precipitation is characterized by extensive spatial coverage, weak precipitation intensity, and minimal upward motion (Yang, Liu, & Yang, 2019).
UHI is a local urban phenomenon that alters the thermal balance and, mostly affects convective precipitation. The UHI causes an updraft over the urban area, increasing moist convection, water vapour

content, and cloud fraction, which increases precipitation (Steensen et al., 2022). This phenomenon is also termed 4'O clock rainfall, which is mainly seen in tropical regions of the northern hemisphere. UHI-induced precipitation was first documented by Landsberg (1956) in Tulsa, Oklahoma (Dixon & Mote, 2003). Convective systems significantly affect the atmosphere's thermal equilibrium and thermodynamic differences, which results in varied moisture cycling, latent heat distribution, cold rain, and warm rain processes, and these variations affect the cloud duration and climate of the Earth (Yanai et al., 1972; Biggerstaff & Listemaa, 2000; Lolli et al., 2017). This can negatively impact numerous economies and age groups susceptible to the effects of climate change (Cui et al., 2022; Motanya & Valera, 2016). Maximum summer precipitation is influenced by solar heating and UHI in the afternoon and by UHI in the evening. This accelerates the destabilization of the low-level atmosphere and increases the frequency of convective precipitation. (Ganeshan et al., 2013). Several studies have examined warm-season rainfall modification over metropolitan areas in the past. One of the earliest studies of a substantial upwind rainfall increase in the La Porte area east of Chicago was conducted by Changnon in 1968. Similar rainfall increases noticed over and downwind of several cities have been mostly linked to the UHI (Ackerman et al., 1977; Bornstein & Lin, 2000; Shepherd et al., 2002; Dixon & Mote, 2003; Shepherd & Burian, 2003; Bentley et al., 2010).

In summer, the intensities of the urban heat islands are positively connected with the amount of precipitation. The Bowen ratio impacts in the summer and the Bowen ratio and snow albedo effect in the winter make rural temperatures susceptible to changes in precipitation (Gu & Li, 2018). The effect of UHI on precipitation is also influenced by urban geography. UHI-affected rainfall is observed in inland cities in the late afternoon and early evening, and it intensifies in the downwind direction of the city. As per the findings of this study, a minor temperature elevation of 5.6% within the urban area resulted in an average monthly increase in rainfall rate of approximately 28% within a distance ranging from 30 to 60 km downwind of the metropolitan region. Increases of up to 51% can be seen in some downwind areas. In addition, it was discovered that the maximum rainfall rates in the downwind affected area were 48%–116% higher than the upwind control area's mean value. The maximum value was often discovered at a typical distance of 64 km from the city's centre or 39 km from the boundary of the urban area (Shepherd et al., 2002). Rainfall in coastal cities impacted by UHI is seen during diurnal hours. Due to the interaction between UHI and sea breeze, there may be a localized increase in the frequency and severity of extreme positive rainfall anomalies during the day (Chagnon et al., 1977; Lin & Chen, 2011; Chakravarty & Bhangale,2021; Chakravarty et al., 2021). Even the formation of clouds and thunderstorms might result from the interaction between UHI and sea breeze (Ihadua & Filho, 2021). Precipitation can aggravate the difference in soil moisture between urban and rural locations, resulting in an increase in SUHII during the day and a decrease in SUHII at night (Li, Zha, & Wang, 2020). Assessment of the exposure of precipitation extremes in response to UHI, however, has received less attention to date.

### *1.3.Population and Precipitation*

In terms of precipitation and heat waves, the number of extreme events caused by global warming is increasing, and they are expected to continue to worsen in the future (Myhre et al., 2019). The growing population and urbanized areas are greatly threatened by these events. This growing threat to the population is quantified by extreme precipitation events (EPEs) in terms of extreme precipitation days and amounts (Risser & Wehner, 2017). Exposure to extreme precipitation events is determined by multiplying the population in the area prone to extreme precipitation events (Jones et al., 2015). In terms of population exposure to EPEs, Zhao et al., (2021) discovered that at 1.5 ℃, 2 ℃, and 3 ℃ warming levels, population exposure to EPEs is anticipated to increase by 72.4%, 122.7%, and 87.6% respectively. In a study conducted in the Yangtze River Delta region and documented by Shen et al. (2022), from 1961 to 2018, all indices related to extreme precipitation events (EPEs) exhibited an increasing trend. Specifically, during the period from 1984 to 1993 compared to the later period from 1994 to the present, the population's exposure to extreme precipitation events, both in terms of daily, daytime, and nocturnal occurrences as well as the corresponding precipitation amounts, witnessed respective increases of 37% (40%), 34% (39%), and 41% (41%) within the timeframe of 2009 to 2018. Furthermore, utilizing simulations derived from the Coupled Model Intercomparison Project phase 6, incorporating Shared

Socioeconomic Pathways and Representative Concentration Pathways, it was determined that the likelihood of extreme precipitation events exceeding the threshold of the 99th percentile is projected to rise globally across all land areas during the upcoming century. This trend is particularly notable under the SSP5-8.5 no-mitigation scenario. According to this scenario, the occurrence of severe precipitation events worldwide is anticipated to increase by approximately 1.8 times by the end of the current century. Even if early mitigation is carried out using SSP1-2.6, increases are still anticipated, but they are considerably less than SSP5-8.5 (Tang & Hu, 2022). Also, under SSP5-8.5, future global aggregate exposure would rise by at least 50% (Chen & Sun, 2021).

Considering future threats to the increasing population due to unpredicted events, the relationship between UHI, population density, and precipitation needs to be studied**.** This study examines the interrelationship among UHI, population density, and unanticipated precipitation events during the summer and winter in Western Coastal Cities. This research employs hypothesis testing to assess this interrelation. The null hypothesis assumes that there is no correlation between the study parameters, whereas the alternative hypothesis assumes that there is a correlation between the study parameters.

## *2. Methodology and Tools*

The physiographic region of India was studied and the region that receives the highest precipitation (figure 2) i.e. The western coastal area is considered (Suthinkumar et al., 2019). Tier 2 cities (also called "Y" class cities) in the Western Coastal area as per the seventh pay commission are taken for further analysis (figure 3). Data such as population density, surface temperature, and precipitation of these selected tier 2 cities were collected (Figure 1).

To examine the unpredictability of events and shifts in trends over time, the study period is delimited to the summer and winter seasons of 1991, 2001, 2011, and 2021. Population data are gathered from census records for the years 1991, 2001, and 2011, while a population projection method known as the geometric increase method is employed to estimate the population for the year 2021 due to the unavailability of the 2021 census.

According to the Koppen climate classification, the summer season for the Indian west coast encompasses the months of March, April, and May, while the winter season encompasses November, December, and January. Surface temperature and precipitation datasets are sourced from the NASA Data Access Viewer portal. For the specified study years, monthly data on precipitation and surface temperature are procured from the portal. These data are then averaged separately for the summer and winter seasons. The collected and processed data is used for further analysis.

The analysis continues with the execution of a hypothesis test to determine the presence or absence of correlations among the chosen parameters (Figure 1). Spearman's rank correlation coefficient is employed to quantify the correlation between surface temperature, population density, precipitation, and humidity. This correlation is explored in terms of its fluctuation over the specified study period. The findings from this analysis will facilitate the drawing of meaningful inferences regarding the relationships and trends among these variables.

The collected data are processed and analyzed using Microsoft Excel software. To establish the correlation between variables, Spearman's rank correlation coefficient is employed. The rationale behind selecting this coefficient is the fact that the dataset under examination exists in a continuous form, which implies that it is measurable and quantitative. To study the relationship between parameters within the context of continuous data, correlation tests are used. Given that the primary objective of this research is to evaluate the extent of association between two variables, noteworthy correlation tests include the Pearson and Spearman correlation coefficients. Because Spearman's rank correlation coefficient is robust against the influence of outliers, this correlation coefficient is employed.

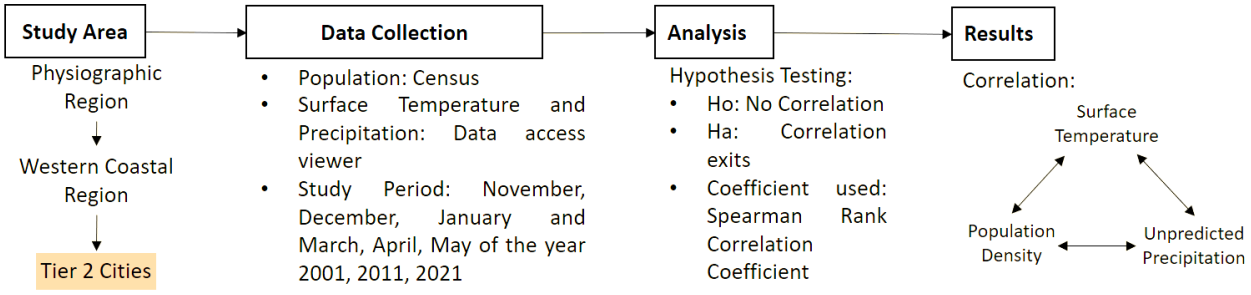


**Figure 1.** Methodology.

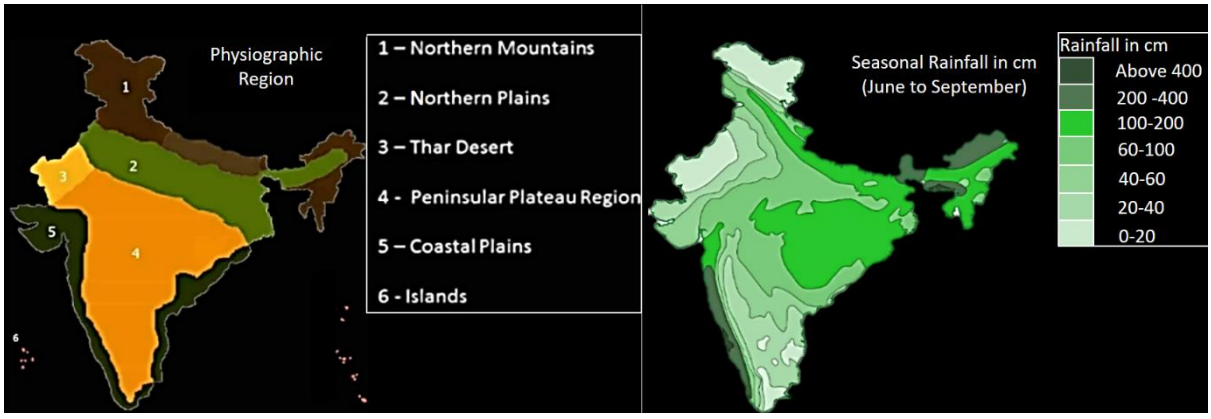


**Figure 2.** Physiographic region and rainfall distribution (Suthinkumar et al., 2019)

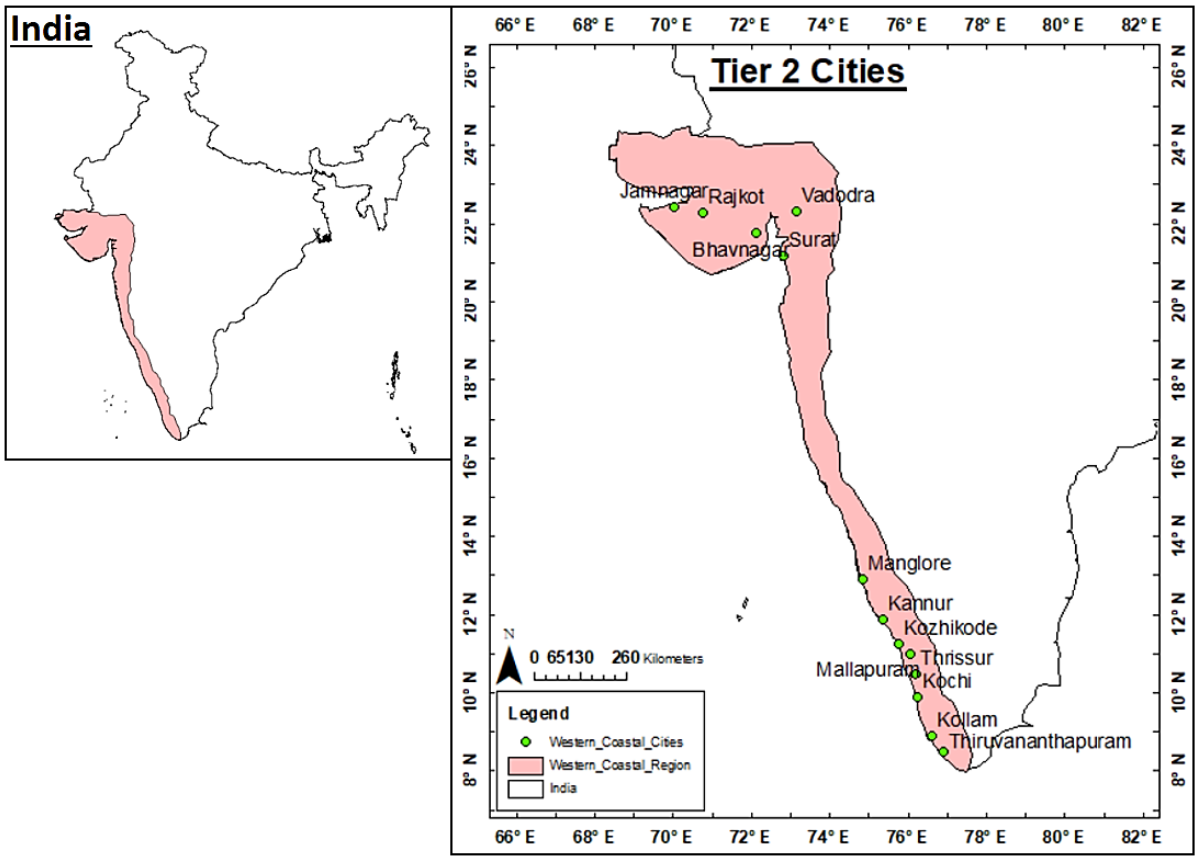


**Figure 3.** Study area.

**Table 1.** Cities data.

| Sr. no. | Cities | Population | Area (sq. Km) | PD (Pop/sq. Km) | Average Summer Temp (° C) | Rainfall (mm) |
|---|---|---|---|---|---|---|
| 1 | Surat | 4467797 | 326.5 | 13721 | 33.14 | 1243 |
| 2 | Kochi | 602046 | 94.8 | 6345 | 29.9 | 3014 |
| 3 | Bhavnagar | 593368 | 67.5 | 9681 | 34.7 | 656 |
| 4 | Vadodara | 1670806 | 219 | 7629 | 34.07 | 846 |
| 5 | Rajkot | 1323363 | 104 | 12725 | 32.7 | 676 |
| 6 | Mangalore | 488968 | 132.4 | 3691 | 29.77 | 3548 |
| 7 | Kannur | 56823 | 78 | 5152 | 27.25 | 3320 |
| 8 | Thrissur | 315957 | 101.5 | 3112 | 29.65 | 3123 |
| 9 | Kolam | 349556 | 57.3 | 6090 | 27.64 | 2427 |
| 10 | Kozhikode | 608255 | 118.5 | 5129 | 28.84 | 2011 |
| 11 | Jamnagar | 600943 | 122 | 4925 | 30.5 | 616 |
| 12 | Thiruvanantha puram | 960437 | 214.8 | 4470 | 29.15 | 1835 |
| 13 | Malappuram | 101386 | 58.2 | 1743 | 27.6 | 2852 |

Tier 2 cities have been selected for in-depth analysis, focusing on key parameters which include population density, temperature, and rainfall. Among, these cities, Surat emerged with the highest population, of approximately 4,467,797 individuals as per the 2011 census (Table 1). This high population is accompanied by a notable population density of 13,721 persons/ $Km^2$, indicating a concentrated urban environment. This indicates that Surat city is highly densified when compared to other cities. High population density can make the city more vulnerable to extreme and unpredictable events, such as natural disasters or public health crises. When many people live close together, the impact of such events can be more significant. A densely populated city like Surat may put more strain on natural resources, including water, energy, and land. Managing these resources sustainably becomes a critical concern.

For temperature-related data during the Summer season, Bhavnagar stands out among the thirteen cities for its distinct characteristics. Specifically, Bhavnagar registered the highest average summer temperature, reaching approximately 34.7 °C (Table 1). This data point underscores the region's propensity for elevated temperatures during summer. High summer temperatures can affect the well-being of residents, potentially leading to heat-related health issues. Adequate cooling and access to clean water becomes essential during hot summers. Elevated temperatures often lead to increased energy consumption for cooling, which can strain the local energy infrastructure.

Considering the precipitation data among the selected cities, Mangalore holds a noteworthy position. Mangalore receives the highest amount of precipitation among the thirteen cities, measuring approximately 3548 mm. This considerable level of rainfall signifies the region's distinct propensity to experience substantial precipitation events. This substantial amount of rainfall indicates the region's unique susceptibility to significant precipitation events, which can influence water resource management, flood risk, and local agriculture. The region's high precipitation levels can influence water resource management. Proper drainage systems and water storage facilities are essential to manage this abundance of water effectively. High levels of precipitation can increase the risk of floods, especially if the city's infrastructure and drainage systems are not well-prepared to handle excessive rainwater. Excessive rainfall can impact local agriculture, potentially leading to issues such as waterlogged fields, crop damage, and challenges in crop planning and cultivation.

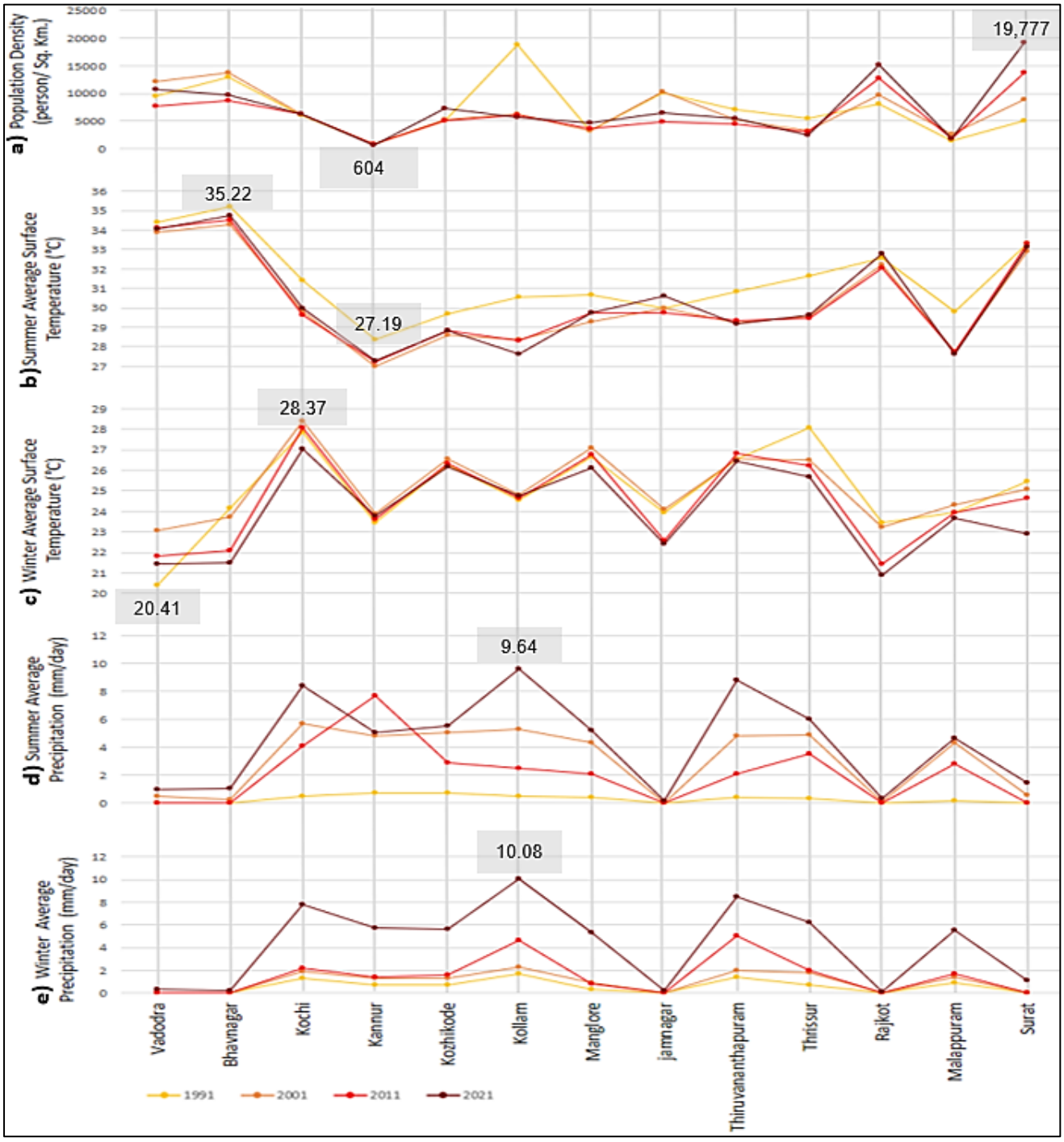


**Figure 4.** Data of selected cities for the years 1991, 2001, 2011 and 2021 related to **a)** population density (person/ sq. Km); **b)** summer average surface temperature (°C); **c)** winter average surface temperature (°C); **d)** summer average precipitation (mm/day) **e)** winter average precipitation (mm/day).

Surat and Rajkot show an increase in population density over time (Figure 4. a). Whereas, in other cities, due to a lower growth rate of population or expansion of city limits, the densities either reduced or remained constant. In the case of Kollam, as the area increased from 18.48 $Km^2$ to 57.31 $Km^2$, a drastic drop in density can be seen from 1991 to 2021 (Kovoor & Panjikaran, 2021). Surat, which is expected to have 62,44,354 populations in 2021, has the highest population density at 19,177 persons/ $Km^2$. The average temperatures in summer and winter are 33.31°C and 24.66°C, respectively, and the average precipitation in summer and winter is 1.43 mm/day and 1.15 mm/day, respectively (Table 2). Kannur, which is expected to have a population of 47,082 in the year 2021, has a lower population density of 604

person/Km$^2$ because of its negative growth rate of 1.1 %. The average temperatures in summer and winter are 27.19°C and 23.60°C, respectively, and the average precipitation in summer and winter is 5.05 mm/day and 5.70 mm/day, respectively (Table 2).

Among the recorded average summer surface temperatures, Bhavnagar recorded the highest temperature in 1991, around 35.22°C (Figure 4. b). Its population density in 1991 was 18,080 persons/ Km$^2$ and Its average annual precipitation in both summer and winter was zero (Table 2). Kannur recorded the lowest average summer surface temperature, 27.00°C in 2001 (Figure 4. b). Among the recorded average winter surface temperatures, Kochi recorded the highest temperature in 2001, around 28.37°C (Figure 4. c). Its population density in 2001 was 6,286 person/ Km$^2$, and its average precipitation in summer and winter was 5.71 mm/day, and 1.88 mm/day, respectively (Table 2). Vadodara recorded the lowest average temperature of, 20.41°C in 1991 (Figure 4. c). Its population density in 1991 was 9,527 persons/ Km$^2$ and Its average annual precipitation in both summer and winter was zero (Table 2).

In summer as well as winter, the highest recorded average precipitation is in Kollam in the year 2021 which is 9.64 mm/day (Figure 4.d) and 10.08 mm/day (Figure 4. e) respectively. Its population density in 2021 is 5,628 person/ Km$^2$, and its average temperature in summer and winter is 27.64°C, and 24.72°C, respectively (Table 2).

**Table 2.** Comparative analysis of cities with the highest and lowest values of key indicators.

| Cities | Year | Population Density (Person/ Km$^2$) | Average Summer Surface Temperature (°C) | Average Winter Surface Temperature (°C) | Average Summer Precipitation (mm/ day) | Average Winter Precipitation (mm/day) |
|---|---|---|---|---|---|---|
| Surat | 2021 | 19,777 | 33.31 | 24.66 | 1.43 | 1.15 |
| Rajkot | 2021 | 15,231 | 32.78 | 20.87 | 0.35 | 0.15 |
| Kannur | 2021 | 604 | 27.19 | 23.60 | 5.05 | 5.70 |
| Bhavnagar | 1991 | 18,080 | 35.22 | 24.12 | 0.00 | 0.00 |
| Kochi | 2001 | 6,286 | 29.79 | 28.37 | 5.71 | 1.88 |
| Vadodara | 1991 | 9,527 | 34.40 | 20.41 | 0.00 | 0.00 |
| Kollam | 2021 | 5,628 | 27.64 | 24.72 | 9.64 | 10.08 |

## 3. Results

The Spearman rank correlation coefficient is a statistical measure used to investigate the relationship between selected parameters, i.e., surface temperature, population density, and precipitation. It offers insights into how these factors co-variate over a given period. By calculating the correlation coefficient, researchers can determine the strength and direction of the relationship between UHI and the other parameters. A positive correlation indicates that as one parameter increases, the other also increases. Conversely, a negative correlation suggests an inverse relation, where one parameter increases and the other decreases. The analysis conducted over a specific time frame allows researchers to assess variations in the relationship between these parameters. This provides valuable information regarding the impact of one parameter on the other over time. The obtained correlation coefficients provide numerical values that quantify the strength and direction of these relations. Positive values close to 1 indicate a strong positive correlation, whereas negative values close to -1 signify a strong negative correlation. Values close to 0 indicate weak or negligible correlation. These correlation coefficients serve as quantitative measures, enabling researchers to assess the impact of surface temperature, population density, and precipitation on the UHI phenomenon. By analysing these coefficients over time, trends and patterns can be identified, aiding in understanding the complex interactions and dynamics between these factors. This information is highly valuable for urban planners, policymakers, and researchers seeking to mitigate the effects of UHI and create more sustainable and resilient cities.

### *3.1. Surface Temperature and Population Density*

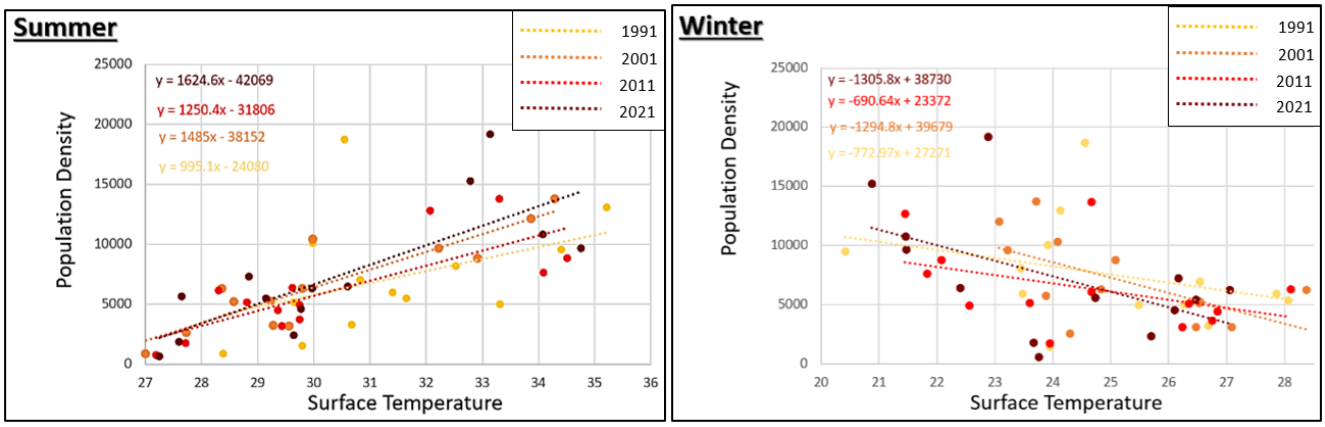


**Figure 5.** Graph illustrating the relationship between surface temperature (°C) and population density (Person/Km$^2$).

**Table 3.** Spearman Rank Correlation Coefficient.

| Surface Temperature and Population Density | | | | |
|---|---|---|---|---|
| **Year** | **Coefficient (Summer)** | **Remark** | **Coefficient (Winter)** | **Remark** |
| **1991** | 0.313 | Weak Positive Association | -0.374 | Weak Negative Association |
| **2001** | 0.741 | Strong Positive Association | -0.621 | Strong Negative Association |
| **2011** | 0.621 | Strong Positive Association | -0.451 | Moderate Negative Association |
| **2021** | 0.802 | Very Strong Positive Association | -0.505 | Moderate Negative Association |

The investigation reveals a distinct seasonal pattern in the relationship between surface temperature and population density within the designated study years of 1991, 2001, 2011, and 2021. During the summer, a positive correlation was observed between surface temperature and population density, indicating that as population density increases, surface temperature also increases. Conversely, in the winter, a negative correlation is evident, signifying that as population density increases, surface temperature decreases (Figure 5).

In summer, the strength of the association between surface temperature and population density gradually intensifies over the years. This is exemplified by the correlation coefficient, a measure of the degree of correlation. In 1991, the correlation coefficient was relatively weak at 0.313, but it substantially increased, reaching 0.802 by 2021 (Table 3). This substantial boost in the correlation coefficient signifies a more pronounced and robust correlation between population density and surface temperature during the summer season, implying that as cities become more densely populated, their impact on local temperatures in the summer becomes increasingly significant.

On the other hand, the winter season does not exhibit a similar trend of strengthening correlation between surface temperature and population density. The relationship remains relatively stable across the study years, indicating that population density's influence on winter temperatures remains consistent. This may be due to the stability of heating practices and a lesser impact of urbanization on winter temperatures compared to the summer. These findings provide valuable insights into the complex interplay between urbanization and climate patterns, with potential implications for urban planning, energy consumption, and sustainability efforts.

### *3.2. Surface Temperature and Precipitation*

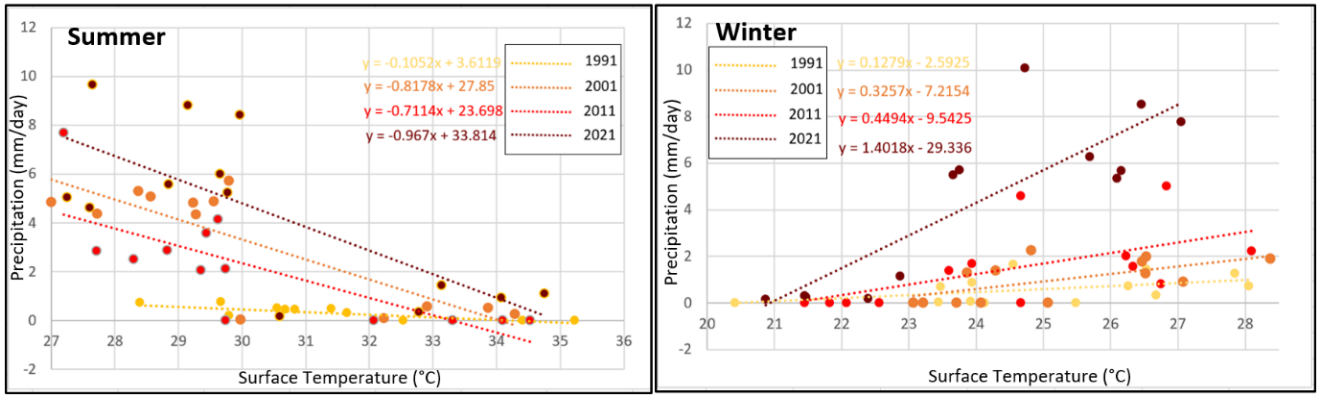


**Figure 6.** Graph illustrating the relationship between surface temperature (°C) and precipitation (mm/day).

**Table 4.** Spearman Rank Correlation Coefficient.

| Surface Temperature and Precipitation | | | | |
|---|---|---|---|---|
| **Year** | **Coefficient (Summer)** | **Remark** | **Coefficient (Winter)** | **Remark** |
| **1991** | -0.635 | Strong Negative Association | 0.511 | Moderate Positive Association |
| **2001** | -0.621 | Strong Negative Association | 0.638 | Strong Positive Association |
| **2011** | -0.740 | Strong Negative Association | 0.713 | Strong Positive Association |
| **2021** | -0.588 | Moderate Negative Association | 0.813 | Very Strong Positive Association |

A distinct connection between surface temperature and precipitation, exhibiting seasonal variation during the summer and winter is observed. During the summer, a negative correlation exists between surface temperature and precipitation (Figure 6). However, this negative correlation has displayed a tendency to wane over the selected study years. This trend is evident through the decreasing coefficient values indicating decreasing association, which have gradually declined from -0.635 in 1991 to -0.588 in 2021 (Table 4).

Conversely, the relationship between surface temperature and precipitation in the winter season is characterized by a positive correlation, and this association has been growing more robust over time, as observed from the study of the selected study period. This escalating association was observed through the ascending coefficient values. This progression signifies an increasingly pronounced positive link between surface temperature and precipitation during winter.

### *3.3. Population Density and Precipitation*

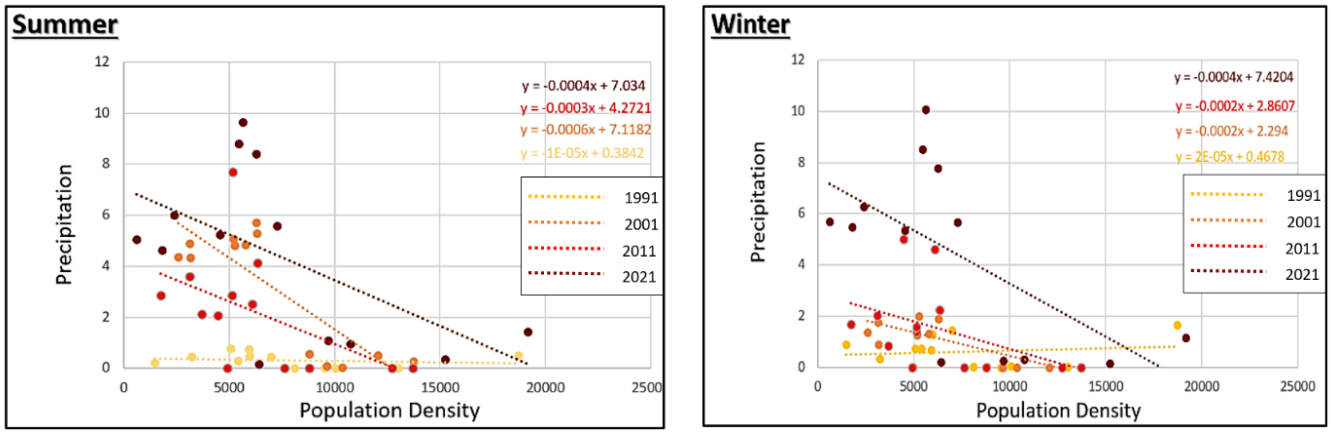


**Figure 7.** Graph illustrating the relationship between population density (Person/Km$^2$) and precipitation (mm/day).

**Table 5.** Spearman Rank Correlation Coefficient.

| Population Density and Precipitation | | | | |
|---|---|---|---|---|
| **Year** | **Coefficient (Summer)** | **Remark** | **Coefficient (Winter)** | **Remark** |
| **1991** | -0.287 | Weak Negative Association | -0.115 | Very weak negative Association |
| **2001** | -0.571 | Moderate Negative Association | -0.646 | Strong Negative Association |
| **2011** | -0.442 | Moderate Negative Association | -0.578 | Moderate Negative Association |
| **2021** | -0.495 | Moderate Negative Association | -0.582 | Moderate Negative Association |

The correlation between population density and precipitation exhibits a negative pattern during both summer and winter (Figure 7). Notably, this negative correlation becomes more pronounced during the summer months, which is evident from the escalating coefficient values observed over the course of the chosen study period (Table 5). However, this trend of strengthening correlation is not evident during the winter.

Considering the null hypothesis (Ho) as no correlation exists between UHI, population density and precipitation. Alternative Hypothesis (Ha) as correlation exists between selected indicators. For the level of significance of 5% and the number of samples 13 (number of cities = 13), $r_c$ is 0.478. This critical value of $r_c$ is compared with the results of the analysis:

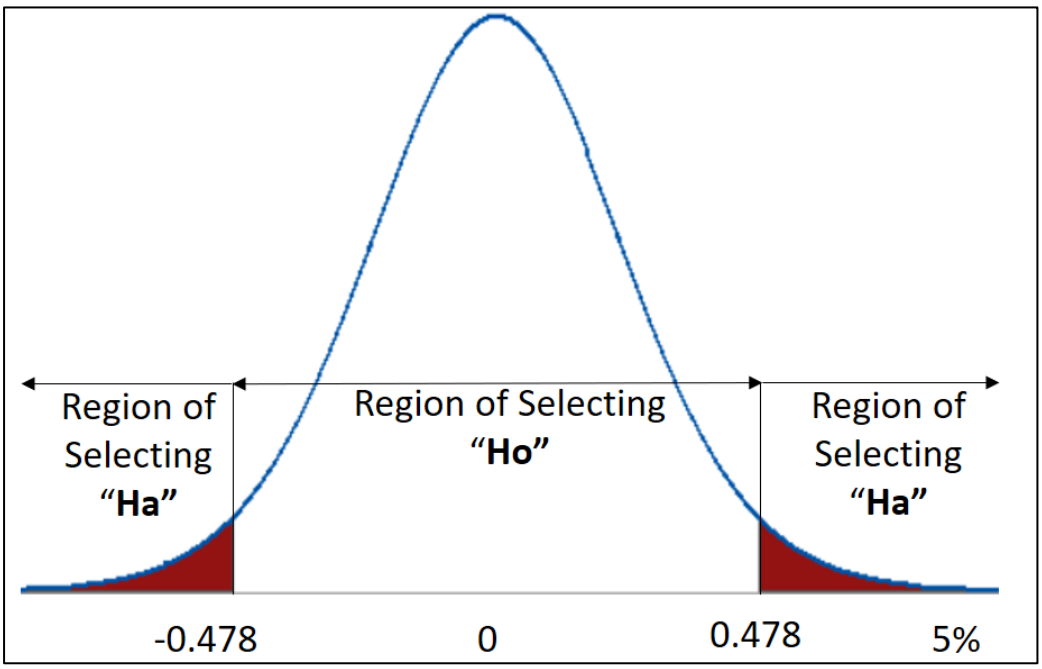


**Figure 8.** Critical Value of Correlation Coefficient.

**Table 6.** Table showing theory's acceptability in terms of accepted hypotheses.

| a. Surface Temperature and Population Density | | | | |
|---|---|---|---|---|
| **Year** | **Summer** | **Hypothesis Accepted** | **Winter** | **Hypothesis Accepted** |
| **1991** | 0.313 | Ho | -0.374 | Ho |
| **2001** | 0.741 | Ha | -0.621 | Ha |
| **2011** | 0.621 | Ha | -0.451 | Ho |
| **2021** | 0.802 | Ha | -0.505 | Ha |

| b. Surface Temperature and Precipitation | | | | |
|---|---|---|---|---|
| **Year** | **Summer** | **Hypo Accepted** | **Winter** | **Hypo Accepted** |
| **1991** | -0.635 | Ha | 0.511 | Ha |
| **2001** | -0.621 | Ha | 0.638 | Ha |
| **2011** | -0.740 | Ha | 0.713 | Ha |
| **2021** | -0.588 | Ha | 0.813 | Ha |
| **c. Population Density and Precipitation** | | | | |
| **Year** | **Summer** | **Hypo Accepted** | **Winter** | **Hypo Accepted** |
| **1991** | -0.287 | Ho | -0.115 | Ho |
| **2001** | -0.571 | Ha | -0.646 | Ha |
| **2011** | -0.442 | Ho | -0.578 | Ha |
| **2021** | -0.495 | Ha | -0.582 | Ha |

The analysis revealed interesting findings regarding the correlation between the selected indicators. First, the acceptance of Ha indicates that a correlation indeed exists among the chosen parameters. Specifically, a positive correlation has been observed between surface temperature and population density during the summer since 2001 (Table 6. a.). This suggests that as population density increases, surface temperatures also tend to rise, indicating a potential urban heat island effect. However, a negative correlation during the winter is inferred from the negative numerical value of the correlation coefficient. However, empirical support for the strength of this relationship remains inconclusive, as per the results of hypothesis testing. Specifically, the null hypothesis is selected for the examined period from 1991 to 2011, whereas the alternative hypothesis is adopted for the timeframe from 2001 to 2021 (Table 6. a). This discrepancy underscores the intricate and unclear nature of the relationship between surface temperature and population density during the winter.

Furthermore, for the correlation between surface temperature and precipitation, a conclusion was drawn from the calculated correlation coefficients. During the summer season, a negative correlation was observed between these variables, whereas in the winter season, a positive correlation was observed. This observation is reinforced by the acceptance of the alternative hypothesis for both seasonal categories throughout the study duration (Table 6. b). This alignment of hypotheses underscores the substantial and noteworthy relationship between surface temperature and precipitation.

When examining the correlation between population density and precipitation, an indistinct negative correlation was observed during the summer. This is elucidated by the acceptance of the null hypothesis for the study period of 1991 and 2011, and the alternative hypothesis for the years 2001 and 2021 (Table 6. c). In contrast, the winter paints a more definitive picture. This is evidenced by the consistent acceptance of the alternate hypothesis across all periods, for the initial year, 1991.

## 4. Discussion

The purpose of this study is to examine the relationship between surface temperature, population density, and precipitation to investigate shifts in traditional seasonal patterns. Previous research has indicated a positive relationship between surface temperature and population density (Oke T. R., 1973; Oke & Maxwell, 1975; Mallick, 2021). However, an intriguing trend surfaced in the context of western coastal cities when scrutinizing the association between population density and surface temperature. During the summer, there is a positive correlation between population density and surface temperature, which has grown stronger over time. This suggests that as population density increases, surface temperatures also climb in these coastal cities during summer, aligning with prior research findings. However, during the winter, a contrasting relationship emerges between population density and surface temperature. Here, a negative correlation exists, indicating that as population density increases in winter, surface temperatures tend to decrease. This finding is captivating and could be linked to distinct factors. During winter, factors such as heating systems, reduced solar radiation, and specific urban features may counteract the urban heat island effect, leading to lower surface temperatures in densely populated regions.

As surface temperatures increase, precipitation also tends to increase (Ackerman et al., 1977; Bornstein & Lin, 2000; Shepherd et al., 2002; Dixon & Mote, 2003; Shepherd & Burian, 2003; Bentley et al., 2010).

In the case of these western coastal cities, a positive correlation was observed between surface temperature and precipitation in the winter season, again aligning with prior research findings. However, a negative correlation was observed between surface temperature and precipitation during the summer.
To understand this discrepancy, it is important to consider the unique geographical characteristics of the study area, particularly its proximity to the ocean. Coastal cities are influenced by the presence of the ocean, resulting in distinct weather patterns and thermal effects. One such effect is the unequal heating of land and water. During the day, land heats up faster than the adjacent ocean, creating a temperature gradient. This temperature difference leads to the formation of sea breezes, which blow from the ocean toward the land. Sea breezes are stronger during the summer when the land surface temperature is higher. This stronger sea breeze can dissipate cloud formation, leading to a negative correlation between the average surface temperature and average precipitation in summer. The cooling effect of the sea breeze reduces cloud formation, resulting in lower precipitation despite higher surface temperatures.
Conversely, during the winter, land breezes occur. Land breezes blow from the land toward the ocean at night when the land surfaces cool down more rapidly than the ocean. This can facilitate the formation of clouds and increase the likelihood of precipitation. As a result, a positive correlation is observed between the average surface temperature and average precipitation in winter when the correlation between population density and surface temperature is negative.
These unique coastal weather patterns and the interplay between land and ocean thermal characteristics contribute to the observed correlations in these western coastal cities. This relationship between surface temperature and precipitation may be a result of these specific geographic and climatic factors. These findings highlight the complexity of studying urban climate dynamics and emphasize the importance of considering local conditions and regional variations when analyzing correlations between urban parameters.

## 5. Conclusion

This study provides a view of the temporal and seasonal correlation between the land surface temperature, population density, and precipitation in the tier 2 Western coastal cities during the study period 1991, 2001, 2011 and 2021. Several conclusions can be drawn from this study.

1. A significant positive relation is observed between surface temperature and population density during summer. This relation is getting stronger over the period, evident from the increasing positive value of the correlation coefficient, from 0.313 in 1991 to 0.802 in 2021 indicating a positive increasing correlation between the parameters. However, an insignificant negative correlation is observed in the winter.
2. The relationship between surface temperature and precipitation is negative for the summer and positive for the winter.
3. The results for the relationship between population density and precipitation suggest that population density and precipitation exhibit unclear seasonal variations in their correlation, indicating the influence of different factors and mechanisms in different seasons. The weak and inconsistent correlation suggests that other factors or regional variations might have a more significant impact on precipitation patterns, which needs to be explored.

Understanding these correlations is crucial for urban planners, policymakers, and researchers to mitigate the urban heat island effect and create more sustainable and resilient urban environments. By considering the relationship between these parameters over time, informed decisions can be made to develop effective strategies to tackle the challenges associated with urbanization, climate change, and population growth.
By dissecting these interactions across seasons and timeframes, a deep understanding of their dynamics emerges. This view aids in making informed decisions regarding urban planning and climate adaptation. Moreover, these insights open avenues for deeper investigations into the mechanisms underlying these complexities. Ultimately, this research enriches our understanding of how these variables intertwine, offering valuable insights for addressing the challenges posed by their interactions.

**Acknowledgements**
We thank the editor who forwarded this paper for review and two anonymous reviewers for their comments on an earlier version of this manuscript. Dr. Meenal Surawar for guidance. Visvesvaraya National Institute of Technology, Nagpur for providing the required infrastructure.

**Funding**
This research did not receive any specific grant from funding agencies in the public, commercial, or not-for-profit sectors.

**Conflicts of Interest**
The Authors declare that there is no conflict of interest.

**Data availability statement**
Data for the analysis is gathered from https://power.larc.nasa.gov/data-access-viewer/.

**Ethics statements**
Studies involving animal subjects: No animal studies are presented in this manuscript.
Studies involving human subjects: No human studies are presented in this manuscript.

**Institutional Review Board Statement**
Not applicable.

**CRediT author statement**
- Conceptualization, Methodology, Project administration, Validation, Visualization, Writing-review: Dr. Meenal Surawar and Phd. Rachana Patil.
- Supervision: Dr. Meenal Surawar.
- Data curation, Formal analysis, Investigation, Resources, Software, Writing – original draft & editing: Phd. Rachana Patil.

**References**
Ackerman, B., Changnon Jr, S. A., Gatz, D. L., Grosh, R. C., Hilbers, S. D., Huff, F. A., Mansell, J. W., OCHS Ill, H. T., Peden, M. E., Schickedanz, P. T., Semonin, R. G., Vogel, J. L., Changnon, S. A., Dzurisin, G., Hilberg F A Huff, S. D., Ochs, H. T., Semohin, R. G., & Vogel Summary, J. L. (1978). Summary of METROMEX, Volume 2: Causes of Precipitation Anomalies Title: Summary of METROMEX. In *METROMEX*, Illinois State Water Survey. http://hdl.handle.net/2142/94633

Arifwidodo, S., & Chandrasiri, O. (2015). Urban heat island and household energy Consumption in Bangkok, Thailand. *Energy Procedia*, *79*, 189–194. https://doi.org/10.1016/j.egypro.2015.11.461

Bentley, M. L., Ashley, W. S., & Stallins, J. (2010). Climatological radar delineation of urban convection for Atlanta, Georgia. *International Journal of Climatology*, *30*(11), 1589–1594. https://doi.org/10.1002/joc.2020

Biggerstaff, M. I., & Listema, S. A. (2000). An Improved Scheme for Convective/Stratiform Echo Classification Using Radar Reflectivity. *Journal of Applied Meteorology*, *39*(12), 2129–2150. https://doi.org/10.1175/1520-0450(2001)040<2129:aisfcs>2.0.co;2

Bornstein, R., and Lin, Q. (2000). Urban heat islands and summertime convective thunderstorms in Atlanta: three case studies. In *Atmospheric Environment*, *34*(3), 507-516. https://doi.org/10.1016/S1352-2310%2899%2900374-X

Chakravarty, K., Bhangale, R., Das, S., Yadav, P., Kannan, B. A. M., & Pandithurai, G. (2021). Unraveling the characteristics of precipitation microphysics in summer and winter monsoon over

Mumbai and Chennai – the two urban-coastal cities of Indian sub-continent. *Atmospheric Research, 249,* 1-14. https://doi.org/10.1016/j.atmosres.2020.105313

Chakravarty, K., Khandare, S., Kumar, N. V. P. K., Bhangale, R., & Maitra, A. (2021). The interseasonal features of precipitation microphysics over Thiruvananthapuram and Kolkata - the two tropical stations of Indian sub-continent. *Journal of Atmospheric and Solar-Terrestrial Physics, 222,* 1-11. https://doi.org/10.1016/j.jastp.2021.105710

Changnon, S. A., Huff, F. A., Schickedanz, P. T., & Vogel, J. L. (n.d.) (1977). *Summary of METROMEX, Volume1: Weather Anomalies and Impacts, 1, Bulletin 62*.

Chen, H., & Sun, J. (2021). Significant Increase of the Global Population Exposure to Increased Precipitation Extremes in the Future. *Earth's Future*, *9*(9). https://doi.org/10.1029/2020EF001941

Cui, Q., Ali, T., Xie, W., Huang, J., & Wang, J. (2022). The uncertainty of climate change impacts on China's agricultural economy based on an integrated assessment approach. *Mitigation and Adaptation Strategies for Global Change*, *27*(3). https://doi.org/10.1007/s11027-022-09999-0

Das, D. N., Chakraborti, S., Saha, G., Banerjee, A., & Singh, D. (2020). Analysing the dynamic relationship of land surface temperature and landuse pattern: A city level analysis of two climatic regions in India. *City and Environment Interactions*, *8*, 1-14. https://doi.org/10.1016/j.cacint.2020.100046

Dissanayake, D., Morimoto, T., Murayama, Y., & Ranagalage, M. (2019). Impact of Landscape Structure on the Variation of Land Surface Temperature in Sub-Saharan Region: A Case Study of Addis Ababa using Landsat Data (1986-2016). *Sustainability (Switzerland)*, *11*(8), 1-18. https://doi.org/10.3390/su11082257

Dixon, G. P., & Mote, T. L. (2003). Patterns and Causes of Atlanta's urban heat sland-Initiated Precipitation. *Journal of Applied Meteorology*, *42*(9), 1273–1284. https://doi.org/10.1175/1520-0450(2003)042<1273:PACOAU>2.0.CO;2

Gabriel, K. M. A., & Endlicher, W. R. (2011). Urban and rural mortality rates during heat waves in Berlin and Brandenburg, Germany. *Environmental Pollution*, *159*(8–9), 2044–2050. https://doi.org/10.1016/j.envpol.2011.01.016

Ganeshan, M., Murtugudde, R., & Imhoff, M. L. (2013). A multi-city analysis of the UHI-influence on warm season rainfall. *Urban Climate*, *6*, 1–23. https://doi.org/10.1016/j.uclim.2013.09.004

Golechha, M., Shah, P., & Mavalankar, D. (2021). Threshold determination and temperature trends analysis of Indian cities for effective implementation of an early warning system. *Urban Climate, 39,* 1-15. https://doi.org/10.1016/j.uclim.2021.100934

Gu, Y., & Li, D. (2018). A modeling study of the sensitivity of urban heat islands to precipitation at climate scales. *Urban Climate*, *24*, 982–993. https://doi.org/10.1016/j.uclim.2017.12.001

Habeeb, D., Vargo, J., & Stone, B. (2015). Rising heat wave trends in large US cities. *Natural Hazards*, *76*(3), 1651–1665. https://doi.org/10.1007/s11069-014-1563-z

Houze, R. A. (1989, April). Observed structure of mesoscale convective systems and implications for large-scale heating. *Quaterly Journal of the Royal Meteorological Society, 115*, 425-461. https://doi.org/10.1002/qj.49711548702

Hwang, Y. H., Nasution, I. K., Amonkar, D., & Hahs, A. (2020). Urban Green Space Distribution Related to Land Values in Fast-Growing Megacities, Mumbai and Jakarta-Unexploited Opportunities to Increase Access to Greenery for the Poor. *Sustainability (Switzerland)*, *12*(12). https://doi.org/10.3390/su12124982

Ihadua, I. M. T. J., & Filho, A. J. P. (2021). On Thunderstorm Microphysics under Urban Heat Island, Sea Breeze, and Cold Front Effects in the Metropolitan Area of Sao Paulo, Brazil. *Atmospheric and Climate Sciences*, *11*(03), 614–643. https://doi.org/10.4236/acs.2021.113037

Jones, B., O'Neill, B. C., Mcdaniel, L., Mcginnis, S., Mearns, L. O., & Tebaldi, C. (2015). Future population exposure to US heat extremes. *Nature Climate Change*, *5*(7), 652–655. https://doi.org/10.1038/nclimate2631

Karsisto, P., Fortelius, C., Demuzere, M., Grimmond, C. S. B., Oleson, K. W., Kouznetsov, R., Masson, V., & Järvi, L. (2016). Seasonal surface urban energy balance and wintertime stability simulated using three land-surface models in the high-latitude city Helsinki. *Quarterly Journal of the Royal Meteorological Society*, *142*(694), 401–417. https://doi.org/10.1002/qj.2659

Ketterer, C., & Matzarakis, A. (2014). Human-biometeorological assessment of the urban heat island in a city with complex topography - The case of Stuttgart, Germany. *Urban Climate*, *10*(P3), 573–584. https://doi.org/10.1016/j.uclim.2014.01.003

Kotharkar, R., & Surawar, M. (2016). Land Use, Land Cover, and Population Density Impact on the Formation of Canopy Urban Heat Islands through Traverse Survey in the Nagpur Urban Area, India. *Journal of Urban Planning and Development*, *142*(1), 04015003. https://doi.org/10.1061/(ASCE)UP.1943-5444.0000277

Kovoor, R. A., & Panjikaran, S. (2022). Analysis on the Strategy of Urban Space Expansion and Land Resource Management. *Journal of Progress in Civil Engineering*, *4*(1), 45-54. https://doi.org/10.53469/jpce.2022.04(01).08

Leroyer, S., Mailhot, J., Bélair, S., Lemonsu, A., & Strachan, I. B. (2010). Modeling the surface energy budget during the thawing period of the 2006 montreal urban snow experiment. *Journal of Applied Meteorology and Climatology*, *49*(1), 68–84. https://doi.org/10.1175/2009JAMC2153.1

Li, L., Zha, Y., & Wang, R. (2020). Relationship of surface urban heat island with air temperature and precipitation in global large cities. *Ecological Indicators*, *117*. https://doi.org/10.1016/j.ecolind.2020.106683

Li, Y., Schubert, S., Kropp, J. P., & Rybski, D. (2020). On the influence of density and morphology on the Urban Heat Island intensity. *Nature Communications*, *11*(1), 1-9. https://doi.org/10.1038/s41467-020-16461-9

Lin, C. Y., Chen, W. C., Chang, P. L., & Sheng, Y. F. (2011). Impact of the urban heat island effect on precipitation over a complex geographic environment in northern Taiwan. *Journal of Applied Meteorology and Climatology*, *50*(2), 339–353. https://doi.org/10.1175/2010JAMC2504.1

Lolli, S., Di Girolamo, P., Demoz, B., Li, X., & Welton, E. J. (2017). Rain evaporation rate estimates from dual-wavelength Lidar measurements and Intercomparison against a model analytical solution. *Journal of Atmospheric and Oceanic Technology*, *34*(4), 829–839. https://doi.org/10.1175/JTECH-D-16-0146.1

Louiza, H., Zéroual, A., & Djamel, H. (2015). Impact of Transport on Urban Heat Island. *International Journal for Traffic and Transport Engineering*, *5*(3), 252–263. https://doi.org/10.7708/ijtte.2015.5(3).03

Malik, K. T., & Gupta, A. (2018, April). Open Green Spaces in Urban Indian Cities, Its Importance, Rapid Decline and Restoration Strategies. *International Journal of Scientific Research and Review*, *7*(4), 178-186.

Mallick, J. (2021). Evaluation of seasonal characteristics of land surface temperature with NDVI and population density. *Polish Journal of Environmental Studies*, *30*(4), 3163–3180. https://doi.org/10.15244/pjoes/130675

Martin, P., Baudouin, Y., & Gachon, P. (2015). An alternative method to characterize the surface urban heat island. *International Journal of Biometeorology*, *59*(7), 849–861. https://doi.org/10.1007/s00484-014-0902-9

Matsumoto, J., Fujibe, F., & Takahashi, H. (2017). Urban climate in the Tokyo metropolitan area in Japan. *Journal of Environmental Sciences*, *59*, 54–62. https://doi.org/10.1016/j.jes.2017.04.012

Mills, G. (2016). *The Climate of London by Luke Howard (1833).* International Association For Urban Climate.

Motanya, N. C., & Valera, P. (2016). Climate Change and Its Impact on the Incarcerated Population: A Descriptive Review. *Social Work in Public Health*, *31*(5), 348–357. https://doi.org/10.1080/19371918.2015.1137513

Myhre, G., Alterskjær, K., Stjern, C. W., Hodnebrog, Marelle, L., Samset, B. H., Sillmann, J., Schaller, N., Fischer, E., Schulz, M., & Stohl, A. (2019). Frequency of extreme precipitation increases extensively with event rareness under global warming. *Scientific Reports*, *9*(1). https://doi.org/10.1038/s41598-019-52277-4

Nuruzzaman, Md. (2015). Urban Heat Island: Causes, Effects and Mitigation Measures - A Review. *International Journal of Environmental Monitoring and Analysis*, *3*(2), 67-73. https://doi.org/10.11648/j.ijema.20150302.15

Ogunjobi, K. O., Adamu, Y., Akinsanola, A. A., & Orimoloye, I. R. (2018). Spatio-temporal analysis of land use dynamics and its potential indications on land surface temperature in Sokoto Metropolis, Nigeria. *Royal Society Open Science*, *5*(12). https://doi.org/10.1098/rsos.180661

Oke, T. R. (1973). City Size and The Urban Heat Island. *Atmospheric Environment*, *7*(8), 769–779. https://doi.org/10.1016/0004-6981(73)90140-6

Oke, T. R., & Maxwell, G. B. (1975). Urban Heat Island Dynamics in Montreal and Vancouver. *Atmospheric Environment*, *9*(2), 191–200. https://doi.org/10.1016/0004-6981(75)90067-0

Oke, T. R., Mills, G., Christen, A., & Voogt, A. (2017). *Urban Climates.* Cambridge University Press. https://doi.org/10.1017/9781139016476

Pal, S., & Ziaul, S. (2017). Detection of land use and land cover change and land surface temperature in English Bazar urban centre. *The Egyptian Journal of Remote Sensing and Space Science*, *20*(1), 125–145. https://doi.org/10.1016/j.ejrs.2016.11.003

Ramamurthy, P., & Bou-Zeid, E. (2017). Heatwaves and urban heat islands: A comparative analysis of multiple cities. *Journal of Geophysical Research*, *122*(1), 168–178. https://doi.org/10.1002/2016JD025357

Ramírez-Aguilar, E. A., Lucas Souza, L. C., Ramírez-Aguilar, E. A., & Lucas Souza, L. C. (2019). Urban form and population density: Influences on Urban Heat Island intensities in Bogotá, Colombia. *Urban Climate*, *29*, 100497. https://doi.org/10.1016/J.UCLIM.2019.100497

Risser, M. D., & Wehner, M. F. (2017, December 12). Attributable Human-Induced Changes in the Likelihood and Magnitude of the Observed Extreme Precipitation during Hurricane Harvey. *Geophysical Research Letters*, *44*(24), 12457-12464. https://doi.org/10.1002/2017GL075888

Russo, A., & Cirella, G. T. (2018). Modern compact cities: How much greenery do we need? *International Journal of Environmental Research and Public Health*, *15*(10). https://doi.org/10.3390/ijerph15102180

Sarbapriya, R., & Ishita, A. (2011). Impact of Population Growth on Environmental Degradation: Case of India. *Journal of Economics and Sustainable Development*, *2*(8), 72-77. ISSN: 2222-1700

Sarkar, A., Saraswat, R. S., & Chandrasekar, A. (1998). Numerical study of the effects of urban heat island on the characteristic features of the sea breeze circulation. *Earth Planet Science*, *2*, 127–137.

Shen, L., Wen, J., Zhang, Y., Ullah, S., Cheng, J., & Meng, X. (2022). Changes in population exposure to extreme precipitation in the Yangtze River Delta, China. *Climate Services*, *27*, 100317. https://doi.org/10.1016/j.cliser.2022.100317

Shepherd, J. M., & Burian, S. J. (2003). Detection of Urban-Induced Rainfall Anomalies in a Major Coastal City. *Earth Interactions*, *7*(4), 1–17. https://doi.org/10.1175/1087-3562(2003)007<0001:douira>2.0.co;2

Shepherd, J. M., Pierce, H., & Negri, A. J. (2002). Rainfall modification by major urban areas: Observations from spaceborne rain radar on the TRMM satellite. *Journal of Applied Meteorology*, *41*(7), 689–701. https://doi.org/10.1175/1520-0450(2002)041<0689:RMBMUA>2.0.CO;2

Simpson, M., Raman, S., Suresh, R., & Mohanty, U. C. (2008). Urban effects of Chennai on sea breeze induced convection and precipitation. *Journal of Earth System Science*, *117*(6), 897–909. https://doi.org/10.1007/s12040-008-0075-1

Steensen, B. M., Marelle, L., Hodnebrog, & Myhre, G. (2022). Future urban heat island influence on precipitation. *Climate Dynamics*, *58*(11–12), 3393–3403. https://doi.org/10.1007/s00382-021-06105-z

Suthinkumar, P. S., Babu, C. A., & Varikoden, H. (2019). Spatial Distribution of Extreme Rainfall Events During 2017 Southwest Monsoon over Indian Subcontinent. *Pure and Applied Geophysics*, *176*(12), 5431–5443. https://doi.org/10.1007/s00024-019-02282-5

Tan, J., Zheng, Y., Tang, X., Guo, C., Li, L., Song, G., Zhen, X., Yuan, D., Kalkstein, A. J., Li, F., & Chen, H. (2010). The urban heat island and its impact on heat waves and human health in Shanghai. *International Journal of Biometeorology*, *54*(1), 75–84. https://doi.org/10.1007/s00484-009-0256-x

Tang, B., & Hu, W. (2022). Significant Increase in Population Exposure to Extreme Precipitation in South China and Indochina in the Future. *Sustainability (Switzerland)*, *14*(10). https://doi.org/10.3390/su14105784

Tran, D. X., Pla, F., Latorre-Carmona, P., Myint, S. W., Caetano, M., & Kieu, H. V. (2017). Characterizing the relationship between land use land cover change and land surface temperature. *ISPRS Journal of Photogrammetry and Remote Sensing*, *124*, 119–132. https://doi.org/10.1016/j.isprsjprs.2017.01.001

Wai, C. Y., Muttil, N., Tariq, M. A. U. R., Paresi, P., Nnachi, R. C., & Ng, A. W. M. (2022). Investigating the relationship between human activity and the urban heat island effect in Melbourne and four other international cities impacted by COVID-19. *Sustainability (Switzerland)*, *14*(1). https://doi.org/10.3390/su14010378

Xiao, J., Spicer, T., Jian, L., Yun, G. Y., Shao, C., Nairn, J., Fawcett, R. J. B., Robertson, A., & Weeramanthri, T. S. (2017). Variation in population vulnerability to heat wave in Western Australia. *Frontiers in Public Health*, *5*. https://doi.org/10.3389/FPUBH.2017.00064

Yamato, H., Mikami, T., & Takahashi, H. (2017). Impact of sea breeze penetration over urban areas on midsummer temperature distributions in the Tokyo Metropolitan area. *International Journal of Climatology*, *37*(15), 5154–5169. https://doi.org/10.1002/joc.5152

Yanai, M. E. S. C. J.-Hwa. (1972). Determination of Bulk Properties of Tropical Cloud Clusters from Large Scale Heat and Moisture Budgets. *Journal of The Atmospheric Sciences*, *30*, 611–627. https://doi.org/10.1175/1520-0469(1973)030<0611:DOBPOT>2.0.CO;2

Yang, Z., Liu, P., & Yang, Y. (2019). Convective/Stratiform Precipitation classification using ground-based doppler radar data based on the K-nearest neighbour algorithm. *Remote Sensing*, *11*(19). https://doi.org/10.3390/rs11192277

Zhao, J. T., Su, B. Da, mondal, S. K., Wang, Y. J., Tao, H., & Jiang, T. (2021). Population exposure to precipitation extremes in the Indus River Basin at 1.5 °C, 2.0 °C and 3.0 °C warming levels. *Advances in Climate Change Research*, *12*(2), 199–209. https://doi.org/10.1016/j.accre.2021.03.005

Zhou, X., & Wang, Y. C. (2011). Dynamics of Land Surface Temperature in Response to Land-Use/Cover Change. *Geographical Research*, *49*(1), 23–36. https://doi.org/10.1111/j.1745-5871.2010.00686.x

**How to cite this article:**

Patil, R., & Surawar, M. (2023). Urban Heat Island Impact and Precipitation Patterns in Indian Western Coastal Cities. Journal of Contemporary Urban Affairs, 7(2), 37-55. https://doi.org/10.25034/ijcua.2023.v7n2-3